JAST
Journal of Aerospace Science and Technology

Pages: 73-83 / Vol. 15/ Issue 2 / Summer- Fall 2022

Journal of Aerospace Science and Technology

www:jast.ias.ir

Scientific-Research Article

Three-Dimensional Robust Guidance Law for Reaching Maneuvering Targets Based on Finite-Time Sliding Mode Control

Seyyed Sajjad Moosapour[1] , **Amin Keyvan**[2]
1-2- Department of Electrical Engineering, Faculty of Engineering, Shahid Chamran University of Ahvaz, Ahvaz, Iran

ABSTRACT

Keywords: *Dynamic inversion, Sliding mode control; Finite-time guidance law; Impact angle constraint; Maneuvering targets*

This paper provides academic insight into designing a three-dimensional guidance law that can be utilized to reach maneuvering targets at definite angles. Firstly, the theoretical phenomenon of a conventional dynamic inversion will be addressed, which can be implemented for reaching targets with constant velocity. However, given that this method does not apply to reaching accelerated targets, a combination of the dynamic inversion method and sliding mode control is presented. These mechanisms can impact maneuvering targets with bounded acceleration. Proceeding with the discussion of these observations, an improved form of the proposed controller will be introduced as this method guarantees a finite reaching time. Furthermore, the chattering phenomenon will be analyzed, which is the chief disadvantage of the sliding mode. Given these findings, a second terminal sliding surface will be presented. This approach will generate continuous guidance law while effectively eliminating the chattering problem in the sliding mode mechanism. Finally, the effectiveness of the proposed guidance laws against maneuvering targets will be demonstrated through the application of numerical simulations.

Introduction

The rapid development of aerospace science and interceptor guidance has brought much attention to the design of guidance laws against maneuvering targets. For an array of rationales attacking maneuvering targets proves to be very fundamental. For instance, attacking maneuvering targets is highly pertinent in the military industry. This phenomenon also proves to be fundamental to designing a terminal impact angles guidance law, which enables further destruction of the target. In recent years, much research has been conducted on this subject. An improved form of Proportional navigation guidance law (PNGL) was proposed in [1]. Also, a new optimal guidance law was introduced using a teaching-learning–based optimization (TLBO) algorithm. Based on the establishments presented in [2], an optimal guidance law was inaugurated, which was utilized to attack maneuvering targets based on the Riccati equation. That study provided an analytical solution for this equation considering the impact angle constraints. Reference [3] presented an optimal guidance law for maneuvering targets. First, the kinematic dynamic is

1 Assistant Professor (Corresponding Author) **Email: *** s.moosapour@scu.ac.ir
2 Msc

DOI: 10.22034/jast.2022.295270.1081
Submit: 29. July 2022/ Accepted: 08.Oct. 2022
Print ISSN:2345-3648 Online ISSN: 1735-2134

linearized, and the optimal control law is introduced for the linear model. Reference [4] considered the impact angle constraint and introduced a new adaptive guidance law, which can effectively reach maneuvering targets in a finite time. The main feature of this study is the design of a new simple adaptive nonlinear guidance law and smooth acceleration commands.

The dynamic inversion (DI) method is one of the nonlinear control methods used widely for guidance law design [5]. Several studies have been carried out in this field. For example, an adaptive guidance law is presented based on a combination of DI and a disturbance observer [6]. Reference [7] utilized the dynamic inversion method and PI controller to design the guidance law for attacking maneuvering targets. Moreover, reference [8] attempted to replace the system's dynamics with desired dynamics with the dynamic inversion method. Then, fuzzy logic was adopted to better tune the system's parameters.

Sliding mode control (SMC) is a well-known control method that ensures satisfactory performance for a wide range of dynamic systems (especially nonlinear systems) in the presence of bounded disturbances and uncertainties. The main drawback of the sliding mode control is the chattering phenomenon (high-frequency oscillations) produced due to the discontinuous part of the SMC law. The chattering problem can be very destructive for the controlled system. Much research has been undertaken on applying sliding mode control in the design of guidance law. For example, a finite-time guidance law was introduced based on terminal sliding mode control (TSMC) in the presence of disturbances in reference [9]. This study solved the singularity problem of terminal sliding mode control by proper control law design. Furthermore, In reference [10], an adaptive law was designed to estimate the target acceleration as an unknown disturbance. A guidance law was proposed based on the fast terminal sliding mode control. Also, reference [11] introduced a guidance law based on a novel time-varying sliding mode control. Thus, ensuring that the interceptor can reach the target at the desired impact angle.

Finite-time convergence is one of the influential indexes for guidance problems. Most of the proposed guidance methods achieve asymptotical tracking. This means that it requires infinite time for convergence. However, in recent years some research has been undertaken to examine the finite-time guidance law. For example, two novel nonsingular TSMC-based guidance laws were presented for a rigid spacecraft [12]. This study guaranteed finite-time convergence by adequately designing the sliding surfaces. The proposition of a fast nonsingular TSMC based on a neural network observer for the formation control of the space crafts was examined in reference [13]. This controller avoids the singularity problem and ensures a faster finite-time convergence compared to congenial TSMC. Reference [14] presented a finite-time sliding mode guidance law with impacting angle constraints. Moreover, a linear extended state observer was adopted to estimate the accelerations of the maneuvering target. A second-order terminal sliding mode guidance law was proposed for intercepting maneuvering targets with unknown acceleration bounds in reference [15]. In addition to finite-time convergence, this method also eliminates the undesirable chattering phenomenon without any performance sacrifice. Further, reference [16] designed a new form of finite-time guidance law. This paper also investigates replacing the discontinuing part of the sliding mode with a continuous component, which intent effectively eliminates the chattering dilemma. However, all of the above-introduced guidance laws were designed for two-dimensional dynamics. Three-dimensional guidance laws are much more applicable in comparison with two-dimensional guidance laws. Most studies focus on dividing a Three-dimensional guidance law into two separate two-dimensional engagements [17]. However, this approach will affect the guidance accuracy. There has also been some research conducted on three-dimensional guidance laws. A feedback linearization control approach was employed in reference [18] for designing guidance laws. Then a combined optimal robust control method was introduced to attack maneuvering targets. A novel guidance law was introduced based on a finite time sliding mode control in reference [19]. An adaptive twisting-based three-dimensional guidance law was presented in reference [20] for nullifying the LOS angle tracking errors. Lastly, reference [21] proposed two composite three-dimensional guidance laws based on backstepping control and nonlinear disturbance observers. However, most of the research which has been done on three-dimensional guidance laws failed to consider finite-time convergence and terminal impact angle constraints.

The mentioned studies all agreed on the predominant problems in the sliding mode control mechanism. These problems are the chattering

phenomenon and finite-time convergence. Thus, this paper proposes a dynamic finite-time dynamic inversion-based sliding mode control-based (DFDISMC) guidance law. In this paper, three theorems will be presented. In the first theorem, the dynamic inversion method is applied to design guidance laws, then the combination of this method and the sliding mode control method is presented. The second theorem provides a finite-time DI-based sliding mode guidance law. The third theorem presented in this paper introduces a dynamic finite-time DI sliding mode control-based guidance law by combining a finite-time DI sliding mode control and a second terminal sliding surface. In this instance, a first-order dynamic is obtained for the control input. Therefore, by integrating the derivative of the control signal, a smooth control signal is obtained, and the chattering phenomenon is avoided. The DFDISMC guidance law's main advantages are the dynamic inversion simplicity and the robustness of the sliding mode control. Also, the DFDISMC guidance law addresses the two underlying problems: infinite time convergence and the chattering phenomenon complication.

The main novelties of this paper are summarized as follows:

1- Designing a new guidance law based on the combination of dynamic inversion and sliding mode control.
2- Introducing conditions for the proposed method that ensures finite-time convergence.
3- Eliminating the chattering effect by introducing a second terminal sliding manifold and proposing a dynamic guidance law.
4- The remaining contents of this paper are presented as follows. The problem statement is presented in section 2. Section 3 proposes a finite-time DI sliding mode three-dimensional guidance law. Furthermore, a dynamic DI sliding mode control is designed to handle the chattering problem. Finally, comparative simulations are presented in Section 4.

Problem Statement

In this paper, a three-dimensional interception-target geometry is considered, as shown in Figure 1, where T shows the target and M shows the interceptor.

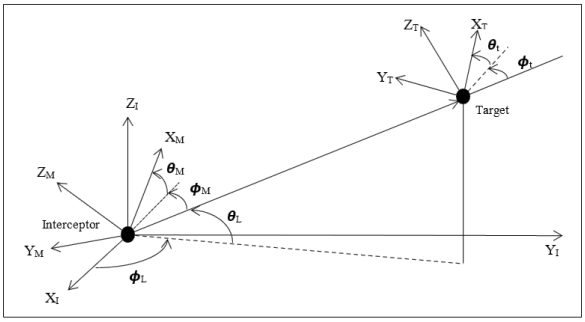

Figure 1. Interceptor-target geometry

In the graphical demonstration presented above, the $X_I Y_I Z_I$ frame is the reference frame and the $X_M Y_M Z_M$ and $X_T Y_T Z_T$ are the velocity frames belonging to the missile and Target, respectively. Furthermore, R is the interceptor and the target relative distance. The symbols V_t and V_m represent the target and the interceptor velocities. Furthermore, a_{ym} , a_{zm} , a_{yt} , and a_{zt} are the yaw and pitch directions for lateral acceleration, which belong to the interceptor and the target respectively. In this model, the interceptor has a constant velocity (V_m) which its direction is defined by angles θ_m and ϕ_m. Also, the target has a constant velocity V_t which is defined by the angles θ_t and ϕ_t respectively. Moreover, θ_L and ϕ_L show the Line of sight (LOS) angles. The three-dimensional dynamics of Figure 1 is shown as follows [22]:

$$\dot{R} = (\rho \cos\theta_t \cos\phi_t - \cos\theta_m \cos\phi_m) V_m \quad (1)$$

$$R\dot{\theta}_L = (\rho \sin\theta_t - \sin\theta_m) V_m \quad (2)$$

$$\dot{\phi}_L R \cos\theta_L = (\rho \cos\theta_t \sin\phi_t - \cos\theta_m \sin\phi_m) V_m \quad (3)$$

$$\dot{\theta}_m = \frac{a_{zm}}{V_m} - \dot{\phi}_L \sin\theta_L \sin\phi_m - \dot{\theta}_L \cos\phi_m \quad (4)$$

$$\dot{\phi}_m = \frac{a_{ym}}{V_m \cos\theta_m} - \dot{\phi}_L \sin\theta_L \cos\phi_m \tan\theta_m - \dot{\theta}_L \sin\phi_m \tan\theta_m - \dot{\phi}_L \cos\theta_L \quad (5)$$

$$\dot{\theta}_t = \frac{a_{zt}}{\rho V_m} - \dot{\phi}_L \sin\theta_L \sin\phi_t - \dot{\theta}_L \cos\phi_t \quad (6)$$

$$\dot{\phi}_t = \frac{a_{yt}}{\rho V_m \cos\theta_t} + \dot{\phi}_L \sin\theta_L \cos\phi_t \tan\theta_t - \dot{\theta}_L \sin\phi_t \tan\theta_t - \dot{\phi}_L \cos\theta_L \quad (7)$$

note that $\rho = \frac{V_t}{V_m}$.

Control objective:

The main objective of this article is to design guidance laws (a_{zm} and a_{ym}) such that θ_L and ϕ_L converge to the desired values and $\dot{\theta}_L$ and $\dot{\phi}_L$ converge to zero.

In this study, R, $\dot{R}$, θ_L, ϕ_L, $\dot{\theta}_L$, $\dot{\phi}_L$, θ_m, and ϕ_m are assumed to be measurable. Besides, θ_{Lf} and ϕ_{Lf} are desired angles, and finally e_1 and e_2 are LOS angle errors and are defined as $e_1 = \theta_L - \theta_{Lf}$ and $e_2 = \phi_L - \phi_{Lf}$.

Assumption 1[23]**:** In the guidance progress, when $R = R_0$, the interception has reached the target. Therefore, R_0 is a very small constant.

Assumption 2: The relative degree between the control inputs and the LOS angles is two and can be written by the following equations.

$$\ddot{\theta}_L = \frac{\cos\theta_t}{R} a_{zt} - \frac{\cos\theta_m}{R} a_{zm} - \dot{\phi}_L^2 \cos\theta_L \sin\theta_L - 2\frac{2\dot{R}\dot{\theta}_L}{R}$$

$$\ddot{\phi}_L = \frac{\cos\phi_t}{R\cos\theta_L} a_{yt} - \frac{\sin\theta_t \sin\phi_t}{R\cos\theta_L} a_{zt} + \frac{\sin\theta_m \sin\phi_m}{R\cos\theta_L} a_{zm} - \frac{\cos\phi_m}{R\cos\theta_L} a_{ym} + 2\dot{\phi}_L\dot{\theta}_L \tan\theta_L - \frac{2\dot{R}\dot{\phi}_L}{R}$$

or in vector form:

$$\ddot{\boldsymbol{\psi}} = \mathbf{F} + \mathbf{B}\mathbf{U} + \mathbf{B_1}\mathbf{D} \qquad (10)$$

where:

$$\ddot{\boldsymbol{\psi}} = \begin{bmatrix} \ddot{\theta}_L \\ \ddot{\phi}_L \end{bmatrix}, \mathbf{F} = \begin{bmatrix} -\dot{\phi}_L^2 \cos\theta_L \sin\theta_L - \frac{2\dot{R}\dot{\theta}_L}{R} \\ 2\dot{\phi}_L\dot{\theta}_L \tan\theta_L - \frac{2\dot{R}\dot{\phi}_L}{R} \end{bmatrix},$$

$$\mathbf{B} = \begin{bmatrix} -\frac{\cos\theta_m}{R} & 0 \\ \frac{\sin\theta_m \sin\phi_m}{R\cos\theta_L} & -\frac{\cos\phi_m}{R\cos\theta_L} \end{bmatrix}, \quad \mathbf{U} = \begin{bmatrix} a_{zm} \\ a_{ym} \end{bmatrix}, \quad \mathbf{B_1} = -\mathbf{B}$$

$$\mathbf{D} = \begin{bmatrix} a_{zt} \\ a_{yt} \end{bmatrix}$$

The important note is that due to the multiplication of **B** in **U**, the LOS can be controlled if $R \neq 0$ and $\theta_m, \phi_m \neq \pm\pi/2$.

Assumption 3: Target accelerations are assumed to be bounded

$|a_{yt}| \le a_1$ and $|a_{zt}| \le a_2$

or

$\mathbf{B_1}\mathbf{D} \le \mathbf{D}_1^*$

In this paper, the inequalities relations for column vectors are defined as follows: If $\mathbf{A} < \mathbf{B}$, the **A** dimension is equal to the dimension of **B** and also all the arrays of **A** are smaller than the same arrays of **B**. Similarly, other relations like ($>$ $=$ and …) are defined.

Also, it is assumed that derivative of the target accelerations are also bounded

$|\dot{a}_{yt}| \le a_3$ and

$|\dot{a}_{zt}| \le a_4$

or

$(\mathbf{B_1}\mathbf{D})' \le \mathbf{D}_2^*$

Guidance Law Design

First, this section presents a guidance law based on the dynamic inversion method, neglecting the target accelerations. The following components present the combination of the DI method with the sliding mode method. Following this, improved forms of this combination are analyzed for designing guidance laws utilizing the three theorems.

Dynamic Inversion Method

Dynamic Inversion is a simple method for controlling dynamic systems [5]. The advantage of this method is its simplicity. However, the disadvantage of this method is its inability to cope with uncertainties and disturbances. In the following equation, the second-order error dynamic is considered:

$$\ddot{\mathbf{E}} + \mathbf{K_v}\dot{\mathbf{E}} + \mathbf{K_p}\mathbf{E} = 0 \qquad (11)$$

where, $\mathbf{E} = \begin{bmatrix} \theta_L - \theta_{Lf} & \phi_L - \phi_{Lf} \end{bmatrix}^T$, $\mathbf{K_v} = 2\xi\omega_n I_{2\times2}$ and $\mathbf{K_p} = \omega_n^2 I_{2\times2}$.

The values of ξ and ω_n can be determined by considering the arbitrary places of poles. It should be noted that the place of the poles should be chosen according to the stability and convergence rate.

Remark 1: Due to the inability of this method in disturbance rejection in dynamics (10), disturbances are neglected, $\mathbf{B_1}\mathbf{D} = [0 \quad 0]$.

Therefore, to achieve equation (11) we adopt the following guidance laws.

$$\mathbf{U}_1 = -\mathbf{B}^{-1}(\mathbf{F} + \begin{bmatrix} \ddot{\theta}_{Lf} \\ \ddot{\phi}_{Lf} \end{bmatrix} + K_v\dot{\mathbf{E}} + K_p\mathbf{E}) \qquad (12)$$

Dynamic Inversion-Based Sliding Mode Control (DISMC)

Despite the effectiveness and simplicity of the dynamic inversion approach, this method cannot eliminate the effects of disturbances. In this case, the

following combinations of the dynamic inversion method with sliding mode control are introduced.

Theorem 1. The following sliding surface is proposed to cope with disturbances. This sliding mode method can easily combine with the dynamic inversion method and allow it to reject disturbances.

The following sliding surface is considered.

$$\mathbf{s} = \mathbf{\Gamma}[\dot{\boldsymbol{\psi}}(t) - \dot{\boldsymbol{\psi}}(t_0) - \int_{t_0}^{t} \ddot{\boldsymbol{\psi}}_{\mathbf{nom}}(\tau) d\tau] = \mathbf{0} \quad (13)$$

Where $\mathbf{\Gamma} = Diag(\Gamma_1, \Gamma_2)$ and Γ_1 , Γ_2 are arbitrary positive gains to be tuned, $Diag(\Gamma_1, \Gamma_2) = \begin{bmatrix} \Gamma_1 & 0 \\ 0 & \Gamma_2 \end{bmatrix}$ and $\mathbf{0}$ is a column vectors consist of zero arrays. $\boldsymbol{\psi}_{\mathbf{nom}}$ is system dynamics (10) neglecting disturbances with nominal guidance law (12). The important feature of the proposed sliding manifold is the existence of $\dot{\boldsymbol{\psi}}(\mathbf{t_0})$ which can eliminate the reaching phase. Therefore, the switching phase can start from the initial time.

The derivative of the sliding surface (13) with respect to time, we have:

$$\dot{\mathbf{s}} = \mathbf{\Gamma}[\ddot{\boldsymbol{\psi}} - \ddot{\boldsymbol{\psi}}_{\mathbf{nom}}] = \mathbf{0} \quad (14)$$

substituting dynamic (10):

$$\dot{\mathbf{s}} = \mathbf{\Gamma}[\mathbf{F} + \mathbf{B}(\mathbf{U_1} + \mathbf{U_2}) + \mathbf{B_1 D} - \mathbf{F} - \mathbf{B U_1}] = 0 \quad (15)$$

where $\mathbf{U_1}$ is the introduced input (12) And the input $\mathbf{U_2}$ is proposed as:

$$Diag(\text{sgn}(\mathbf{s}))\dot{\mathbf{s}} \le -\boldsymbol{\eta} \quad (16)$$

Where, sgn(.) is the sign function which is defined as $sgn(c) = \begin{Bmatrix} 1 & c > 0 \\ 0 & c = 0 \\ -1 & c < 0 \end{Bmatrix}$, and for vectors, $sgn(c) = \begin{bmatrix} sgn(s_i) \\ \vdots \\ sgn(s_n) \end{bmatrix}$ The diagonal matrix of a vector is defined as $Diag(\mathbf{A}) = Diag(a_1, a_2, \ldots, a_n) = \begin{bmatrix} a_1 & 0 & 0 & 0 \\ 0 & a_2 & 0 & 0 \\ 0 & 0 & \ddots & 0 \\ 0 & 0 & 0 & a_n \end{bmatrix}$ and $\boldsymbol{\eta}$ is a vector with positive entries.

Considering the sliding mode condition (16), the input is computed as

$$\mathbf{U_2} = (\mathbf{\Gamma B})^{-1}[-\mathbf{K}\,\text{sgn}(\mathbf{s})] \quad (17)$$

where $\mathbf{K} = Diag(k_1, k_2)$ is a matrix and and $\mathbf{K I}_{2*1} = \mathbf{D}_1^* + \boldsymbol{\eta}$

To investigate the stability, the following Lyapunov function is chosen:

$$\mathbf{V} = \frac{1}{2} Diag(\mathbf{s})\mathbf{s} \quad (18)$$

The Lyapunov function (18) is a positive definite function. The derivative of the Lyapunov function (18) is computed as follows:

$$\dot{V} = Diag(\dot{\mathbf{s}})\mathbf{s} \quad (19)$$

Considering the derivative of sliding surface (15), using equation (16) and the inequality (17):

$$\dot{V} \le -\boldsymbol{\eta}|\mathbf{s}| \quad (20)$$

Where, $|c|$ is the absolute value function of c (constant) and is defined for vector $\mathbf{s}$ as $|\mathbf{s}| = \begin{bmatrix} |s_1| \\ |s_2| \end{bmatrix}$.

Consequently, the Lyapunov stability is proved.

Remark 2: As was previously mentioned, the two fundamental problems with sliding mode control are the chattering phenomenon and infinite time convergence. From the above analysis, it is patent that the sliding mode control method proposed in theorem 1 suffers from both problems.

Finite-time Dynamic Inversion-Based Sliding Mode Control (FDISMC)

In this part, conditions are introduced for dynamic inversion (nominal input) and the sliding mode control that guarantees the finite-time convergence of the controller.

Finite-time control is an important topic in the control of dynamic systems. The system's trajectories converge to an equilibrium point in finite time by designing a finite-time controller.

Lemma 1 [24]**:** consider the following linear system

$$\ddot{x} = u \quad (21)$$

By applying the following control input, the close loop system converges to the origin in finite time.

$$u = -\mu|\dot{x}|^{\alpha} sign(\dot{x}) - \upsilon|x|^{\frac{\alpha}{2-\alpha}} sign(x) \quad (22)$$

with parameters $\upsilon > \mu > 0$ and $\alpha \in [0,1)$.

Lemma 2 [25]**:** Assume that a Lyapunov function $V(t)$ meets the following condition:

$$\dot{V}(t) \le \delta_1 V(t)^{\theta_1/\theta_2} + \delta_2 V(t) \quad for\ t \ge t_0 \quad (23)$$

Where, δ_1 and δ_2 are positive constants. Also, θ_1 and θ_2 are positive odd numbers where, $\theta_1 < \theta_2$. Then, for initial time t_0, the Lyapunov function decreases to zero in finite-time:

$$t_s \le t_0 + \frac{1}{\delta_2 + \theta_1/\theta_2} \ln \frac{\delta_1 + \delta_2 v(t_0)^{1-\theta_1/\theta_2}}{\delta_1} \quad (24)$$

Theorem 2. Considering dynamic (10), the sliding surface (13) and the Lyapunov function (18), the following nominal control input is introduced.

$$\mathbf{U_1} = -\mathbf{B}^{-1}(\mathbf{F} + \begin{bmatrix} \ddot{\theta}_{Lf} \\ \ddot{\phi}_{Lf} \end{bmatrix} + \mu|\dot{\mathbf{E}}|^{\alpha} sign(\dot{\mathbf{E}}) + \upsilon|\mathbf{E}|^{\frac{\alpha}{2-\alpha}} sign(\mathbf{E})) \quad (25)$$

Where, the power of vectors is defined as $\mathbf{V}^{\alpha} = \begin{bmatrix} v_1^{\alpha} & \cdots & v_n^{\alpha} \end{bmatrix}$. After applying control input (25) to equation (10), the following error dynamic is achieved.

$$\ddot{\mathbf{E}} + \mu|\dot{\mathbf{E}}|^{\alpha} sign(\dot{\mathbf{E}}) + \upsilon|\mathbf{E}|^{\frac{\alpha}{2-\alpha}} sign(\mathbf{E}) = 0 \quad (26)$$

According to lemma 1, the control objective of the certain system is met in finite time.
Considering the sliding manifold (13), the following control law is proposed.

$$\mathbf{U_2} = (\Gamma\mathbf{B})^{-1}\left[-\mathbf{K}\,\mathrm{sgn}(\mathbf{s}) + \delta_1 2^{-\theta_1/\theta_2}\mathbf{s}^{(2\theta_1-\theta_2)/\theta_2} + \delta_2 \frac{1}{2}\mathbf{s} \right] \quad (27)$$

By adopting Lyapunov function (18), considering equation (15), and applying proposed control input (27) Where $\mathbf{KI}_{2*1} = \mathbf{D}_1^* + \boldsymbol{\eta} + \delta_1(\frac{1}{2}|\mathbf{s}|)^{\theta_1/\theta_2} + \delta_2 \frac{1}{2}|\mathbf{s}|$, the following inequality is achieved according to lemma 2.

$$\begin{aligned} \dot{\mathbf{V}} &\le -\eta|\mathbf{s}| + \delta_1(\frac{1}{2}\mathbf{s}^2)^{\theta_1/\theta_2} + \delta_2 \frac{1}{2}\mathbf{s}^2 \\ &\le \delta_1(\mathbf{V(t)})^{\theta_1/\theta_2} + \delta_2\mathbf{V(t)} \end{aligned} \quad (28)$$

The system's errors converge to zero in a finite time. Furthermore, the effects of the bounded disturbances and uncertainties are rejected. Thus according to proposed control laws, the error states converge to the sliding manifold in a finite time and then converge to the origin by applying the control input (25) in a finite time.

Dynamic Finite-time Dynamic Inversion-Based Sliding Mode Control (DFDISMC)

Section 3-3 addressed the finite-time tracking problem of the proposed sliding mode control. In this subsection, the chattering problem of sliding mode needs to be solved.
Therefore, in this section of the paper, a second sliding surface is introduced to achieve the first-order control dynamic to eliminate the chattering problem evident in the sliding mode mechanism. Also, the second sliding surface is designed in a terminal form. Then, combining the proposed finite-time dynamic inversion control and the terminal sliding surface, the overall control law would render finite-time stable.

Theorem 3: in this part, the second sliding surface is designed to help generate a dynamic form for the proposed control input that would eliminate the chattering phenomenon.

The second terminal sliding surface is designed as:

$$\boldsymbol{\sigma} = \mathbf{s} + \beta\dot{\mathbf{s}}^{\lambda_1/\lambda_2} = \mathbf{0} \quad (29)$$

Where, β is an adjustment gain chosen as a positive scalar. Also, λ_1 and λ_2 are the positive scalars that are selected as λ_1 and λ_2 are positive odd numbers and $1 < \frac{\lambda_1}{\lambda_2} < 2$.

In equation (29), $\mathbf{s}$ is the proposed sliding surface:

$$\mathbf{s} = \boldsymbol{\Gamma}[\dot{\boldsymbol{\psi}}(t) - \int_{t_0}^{t} \ddot{\boldsymbol{\psi}}_{\mathbf{nom}}(\tau)d\tau] = 0 \quad (30)$$

Then by determining the derivative of equation (30) concerning time and applying finite-time dynamic inversion (25) as a nominal control input, equation (31) is released:

$$\dot{\mathbf{s}} = \Gamma[\mathbf{B}\mathbf{u}_2 + \mathbf{B}_1\mathbf{D}] \quad (31)$$

According to equation (30), the initial values of the system do not need to be specified for designing the sliding mode control. This is based on the last deduction that the proposed nonsingular terminal sliding mode leads errors to the sliding surface (30), then they slide to the origin. Thus, a constant proportional law [26] is proposed for the terminal sliding mode:

$$\dot{\boldsymbol{\sigma}} = -\rho_1\,\mathrm{sgn}(\boldsymbol{\sigma}) - \rho_2\boldsymbol{\sigma} \quad (32)$$

that $\rho_1, \rho_2 > 0$.

The derivative of sliding surface (28) is

$$\dot{\boldsymbol{\sigma}} = \dot{\mathbf{s}} + \beta\frac{\lambda_1}{\lambda_2} Diag(\dot{\mathbf{s}}^{\lambda_1-\lambda_2/\lambda_2})\ddot{\mathbf{s}} = \beta\frac{\lambda_1}{\lambda_2} Diag(\dot{\mathbf{s}}^{\lambda_1-\lambda_2/\lambda_2})(\frac{\lambda_2}{\beta\lambda_1}\dot{\mathbf{s}}^{2-\lambda_1/\lambda_2} + \ddot{\mathbf{s}}) \quad (33)$$

Considering λ_1 and λ_2 in (33), we have [27]

$$\begin{aligned} &\dot{s}^{\lambda_1-\lambda_2/\lambda_2} > 0 \quad \text{for } \dot{s} \ne 0 \\ &\dot{s}^{\lambda_1-\lambda_2/\lambda_2} = 0 \quad \text{for } \dot{s} = 0 \end{aligned} \quad (34)$$

Then, we can replace $\beta\frac{\lambda_1}{\lambda_2} Diag(\dot{\mathbf{s}}^{\lambda_1-\lambda_2/\lambda_2})$ with a positive constant ρ_3 for $\dot{s} \ne 0$

$$\dot{\boldsymbol{\sigma}} = \rho_3(\frac{\lambda_2}{\beta\lambda_1}\dot{\mathbf{s}}^{2-\lambda_1/\lambda_2} + \ddot{\mathbf{s}}) \quad (35)$$

Considering equation (32)

$$\dot{\boldsymbol{\sigma}} = \rho_3(\frac{\lambda_2}{\beta\lambda_1}\dot{\mathbf{s}}^{2-\lambda_1/\lambda_2} + \ddot{\mathbf{s}}) = \rho_1\,\mathrm{sgn}(\boldsymbol{\sigma}) - \rho_2\boldsymbol{\sigma} \quad (36)$$

or

$$\dot{\boldsymbol{\sigma}} = (\frac{\lambda_2}{\beta\lambda_1}\dot{\mathbf{s}}^{2-\lambda_1/\lambda_2} + \ddot{\mathbf{s}}) = -\frac{\rho_1}{\rho_3}\mathrm{sgn}(\boldsymbol{\sigma}) - \frac{\rho_2}{\rho_3}\boldsymbol{\sigma} \quad (37)$$

The equation (37) can be written as:

$$\ddot{\mathbf{s}} = \frac{\rho_1}{\rho_3}\mathrm{sgn}(\boldsymbol{\sigma}) - \frac{\rho_2}{\rho_3}\boldsymbol{\sigma} - \frac{\lambda_2}{\beta\lambda_1}\dot{\mathbf{s}}^{2-\lambda_1/\lambda_2} \quad (38)$$

Also the derivative of equation (31) with respect to time is calculated as:

$$\ddot{\mathbf{s}} = \boldsymbol{\Gamma}\left[\dot{\mathbf{B}}\mathbf{u}_2 + \mathbf{B}\dot{\mathbf{u}}_2 + (B_1\mathbf{d})'\right] \quad (39)$$

Then, the following control law is proposed:

$$\boldsymbol{\Gamma}\mathbf{B}\dot{\mathbf{u}}_2 = -\left[\frac{\lambda_2}{\beta\lambda_1}\dot{\mathbf{s}}^{2-\lambda_1/\lambda_2} + \boldsymbol{\Gamma}\dot{\mathbf{B}}\mathbf{u}_2 + \frac{\rho_1}{\rho_3}\mathrm{sgn}(\boldsymbol{\sigma}) + \frac{\rho_2}{\rho_3}\boldsymbol{\sigma}\right] \quad (40)$$

Proof:

Considering the following Lyapunov function:

$$\mathbf{V} = \frac{1}{2}Diag(\boldsymbol{\sigma})\boldsymbol{\sigma} \quad (41)$$

The derivative of Lyapunov function (41) is

$$\dot{\mathbf{V}} = Diag(\boldsymbol{\sigma})\dot{\boldsymbol{\sigma}} \quad (42)$$

Applying equations (38) and (39), we have:

$$\dot{V} = Diag(\sigma)(\dot{s} + \beta\frac{\lambda_1}{\lambda_2}Diag(\dot{\boldsymbol{s}}^{\lambda_1/\lambda_2})\ddot{\boldsymbol{s}}) = Diag(\boldsymbol{\sigma})(\dot{\boldsymbol{s}} + \boldsymbol{\beta}\frac{\boldsymbol{\lambda_1}}{\boldsymbol{\lambda_2}}Diag(\dot{\boldsymbol{s}}^{\boldsymbol{\lambda_1/\lambda_2}})\boldsymbol{\Gamma}(\dot{\boldsymbol{B}}_{\boldsymbol{u_2}} + \boldsymbol{B}_{\dot{\boldsymbol{u}}_2} + (\boldsymbol{B_1}\,\boldsymbol{d})')) \quad (43)$$

Applying control input (40), we have:

$$\begin{aligned}
\dot{\mathbf{V}} &= Diag(\boldsymbol{\sigma})(\dot{\mathbf{s}} + \beta\frac{\lambda_1}{\lambda_2}Diag(\dot{\mathbf{s}}^{\lambda_1/\lambda_2})\ddot{\mathbf{s}}) = \\
&Diag(\boldsymbol{\sigma})\beta\frac{\lambda_1}{\lambda_2}Diag(\dot{\mathbf{s}}^{\lambda_1-\lambda_2/\lambda_2})(\frac{\lambda_2}{\beta\lambda_1}\dot{\mathbf{s}}^{2-\lambda_1/\lambda_2} + \boldsymbol{\Gamma}\left[\dot{\mathbf{B}}\mathbf{u}_2 + \mathbf{B}\dot{\mathbf{u}}_2 + (B_1\mathbf{d})'\right])) \\
&= Diag(\boldsymbol{\sigma})\left[\beta\frac{\lambda_1}{\lambda_2}Diag(\dot{\mathbf{s}}^{\lambda_1-\lambda_2/\lambda_2})(\left[-\frac{\rho_1}{\rho_3}\mathrm{sgn}(\boldsymbol{\sigma}) - \frac{\rho_2}{\rho_3}\boldsymbol{\sigma} + (B_1\mathbf{d})'\right])\right] \\
&= \frac{\beta\lambda_1}{\lambda_2}Diag(\dot{\mathbf{s}}^{(\lambda_1-\lambda_2)/\lambda_2})(-\frac{\rho_1}{\rho_3}|\boldsymbol{\sigma}| - \frac{\rho_2}{\rho_3}\boldsymbol{\sigma}^2 + \sigma\mathbf{B_1}\mathbf{d}) \\
&\le \frac{\beta\lambda_1}{\lambda_2}\dot{\mathbf{s}}^{(\lambda_1-\lambda_2)/\lambda_2}(-\frac{\rho_1}{\rho_3}|\boldsymbol{\sigma}| - \frac{\rho_2}{\rho_3}\boldsymbol{\sigma}^2 + |\boldsymbol{\sigma}|D_2^*)
\end{aligned} \quad (44)$$

since $\dot{\mathbf{s}}^{(\lambda_1-\lambda_2)/\lambda_2}$ is equal to zero for $\dot{\mathbf{s}} = 0$ and is positive for $\dot{s} \neq 0$, and also because $|D_2^*|$ is bounded, it can be concluded that $\dot{\mathbf{V}}$ is negative definite and therefore the proof is achieved .

Simulations

This section presents numerical simulations to confirm and validate the introduced guidance laws. The simulations in this research have been done using MATLAB/Simulink. Besides, the ODE45 solver has been applied to solve the nonlinear equations. To illustrate the proper performance of the proposed guidance methods, the initial values of the guidance system are as follows.

The initial values of the guidance system are as follows. The interceptor maintains a constant speed, which is $V_m = 850m/s$. In addition, the constant speed of target is $V_t = 850m/s$. The initial distance between interceptor and target is $R(0) = 12000$. The initial elevation angle and azimuth angle of LOS to inertial reference coordinate system are $\theta_L(0) = 30^\circ$ and $\phi_L(0) = 30^\circ$. On the other hand, initial elevation and azimuth angles of the interceptor to LOS coordinate system are $\theta_m(0) = 10^\circ$ and $\phi_m(0) = 10^\circ$. Also, initial elevation and azimuth angles of the target are $\theta_t(0) = 20^\circ$ and $\phi_t(0) = 180^\circ$, and the desired angles are $\theta_{Lf} = 35^\circ$ and $\phi_{Lf} = 5^\circ$.

To examine the effectiveness of the proposed guidance law, the proposed law is compared with PNGL and SMC. The PNGL can be expressed as:

$$\mathbf{U} = \begin{bmatrix} -N_1\dot{R}\dot{\theta}_L \\ -N_2\dot{R}\dot{\phi}_L \end{bmatrix} \quad (45)$$

Where, N_1 and N_2 are tuning constant parameters. The sliding mode control is presented with the following linear surface:

$$\mathbf{S} = \begin{bmatrix} s_1 \\ s_2 \end{bmatrix} = \dot{\mathbf{E}} + \beta\mathbf{E}$$

And the SMC guidance law is designed as:

$$\mathbf{U} = -\mathbf{B}^{-1}(-\mathbf{F} - \mathbf{k}\,\mathrm{sgn}(\mathbf{s})) \quad (46)$$

Where, $\mathbf{k} = diag(k_1, k_2)$ and $\mathbf{k}I_{2*1} > D_1^*$, also the PNGL parameters are selected as $N_1 = 7$ and $N_2 = 7$.

The interceptor cannot provide a large magnitude of acceleration. Therefore, in practice, the actual interceptor acceleration is limited by:

$$a_M = \begin{cases} a_{M\,MAX}\ sign(a_M) & if\ |a_M| \ge a_{M\,MAX} \\ a_M & if\ |a_M| < a_{M\,MAX} \end{cases} \quad (47)$$

Where, $a_{M\,MAX} = 40g$ is the maximum allowable lateral acceleration.

Also, for better comparison, cumulative velocity increment is defined as follows:

$$\Delta v = \int_0^{t_f} a\,dt \qquad (48)$$

To reveal the efficiency of the provided guidance law, we discuss the following two cases.

Case 1: $a_{yt} = a_{zt} = 19.6 m/s^2$

Case 2: $a_{yt}, a_{zt} = 19.6\sin(t) * u(t-4) m/s^2$ where $u(t)$ is the step function

These assumptions are taken into account according to references [28, 29].

The parameters of DFDISMC Guidance law are given in table 1.

Table 1. The DFDISMC guidance law parameters

Parameter	Γ_1	Γ_2	η_1	η_2	α	μ
Value	1	1	2	2	0.5	0.25
Parameter	υ	β	λ_1	λ_2	ρ_1	ρ_2
Value	0.5	2	5	3	2.5	2.5

In this section, the SMC and PNGL methods are chosen for comparison to effectively evaluate the superiority of the proposed guidance law in convergence, speed and accuracy.

Case 1:

In figures. 2-5 the simulation results for the target with accelerations case 1 are presented.

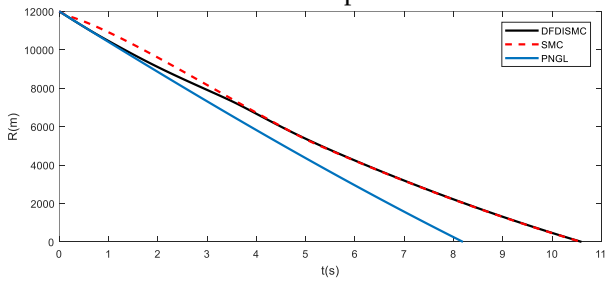

Figure 2. The relative distance between the interceptor and the target

Figure 2 shows the relative distance between the interceptor and target under three guidance laws. The interceptor can successfully reach the target by the three guidance laws, although the interception time is different. As can be seen, the interceptor reaches the target in less than 11 seconds under SMC and DFDISMC laws. Nevertheless, it reaches the target in 7 seconds under the PN guidance law. By comparing the reaching time, the PN guidance law performs better.

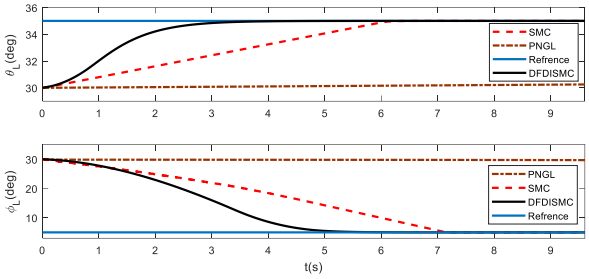

Figure 3. Curves of θ_L and ϕ_L

The angles θ_L and ϕ_L are shown in figure 3. As it can be seen, θ_L and ϕ_L under SMC and DFDISMC guidance laws converge to the reference angles, while these angles under PNGL do not converge to the LOS angles. This is the main drawback of the PN guidance law. Despite the high convergence rate, the LOS angles cannot converge to the desired angles.

By comparing DFDISMC and SMC methods, it is clear that the LOS angles under the DFDISMC guidance law have a faster convergence rate and Better performance than the SMC protocol

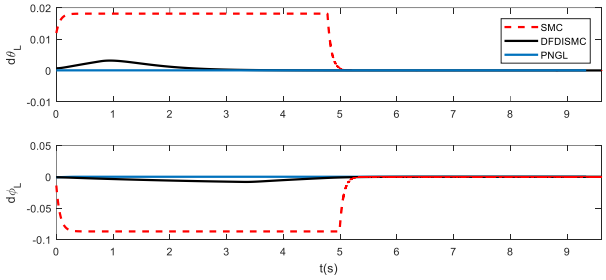

Figure 4. Curves of $\dot{\theta}_L$ and $\dot{\phi}_L$

In Figure 4, the derivative of the angles, θ_L and ϕ_L are presented concerning time. The derivative of the angles should converge to zero. As evident, the derivative of the angles under DFDISMC converges to zero faster and with less error value than the SMC method.

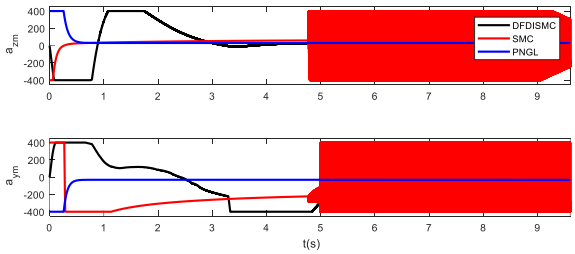

Figure 5. interceptor accelerations

As can be seen in Figure 5, the acceleration of the three guiding rules is within the acceptable range. The acceleration of the PNGL guidance law is very smooth. However, as mentioned, it cannot reach the

target with desired angles. The acceleration of the interceptor under SMC guidance law suffers from the chattering phenomenon, which is visible near collision and is very destructive. Despite the multiple times' entry into the saturation part, the acceleration of the DFDISMC law is smooth. The guidance system purposes are fully met, and the chattering phenomenon is eliminated.

Case 2:

The simulation results are shown in Figures 6-9 for the target with accelerations case2.

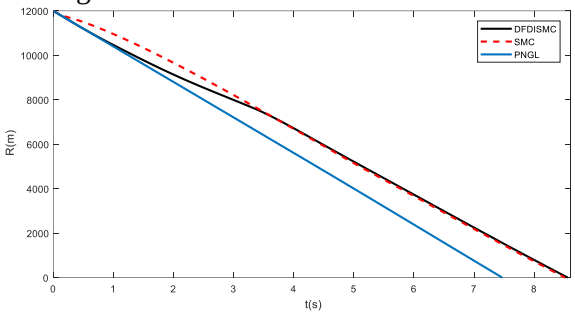

Figure 6. Relative distance curves

Figure 6 shows the relative distance curves between the interceptor and target under three guidance laws. The interceptor reaches the target under all three guidance laws at appropriate times. As in case 1, the interceptor under the PN guidance law reaches the target in less time, and the interceptor reaching time under the SMC and the DFDISMC laws is almost equal.

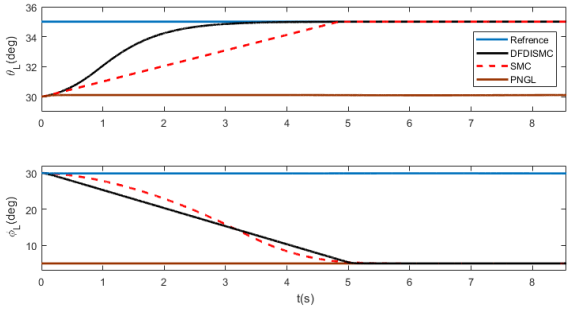

Figure 7. Impact angles θ_L and ϕ_L

It is evident in figure 7 that both SMC and DFDISMC ensure the LOS angles converge to expected values, whereas the PNGL cannot do it. It should be noted that despite the proper performance of methods DIDISMC and SMC, DFDISMC yields better performance and faster convergence.

This figure is crucial as it shows the proper performance of the proposed guidance law and the impact of expected angles on the maneuvering target with variable accelerations.

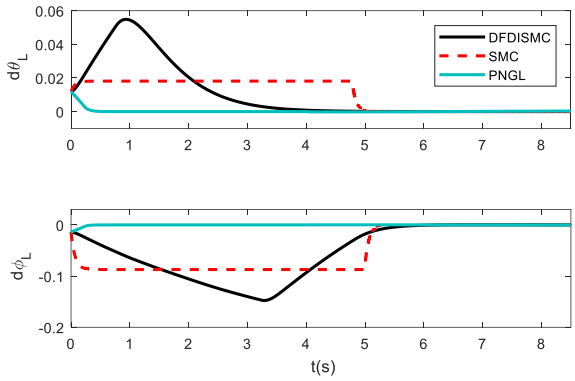

Figure 8. LOS angular rate

Figure 8 shows the LOS angular rates. LOS angular rates should converge to zero. As can be seen, LOS angular rates converge to zero under DFDISMC and SMC guidance laws. However, the convergence rate is faster under the DFDISMC guidance law.

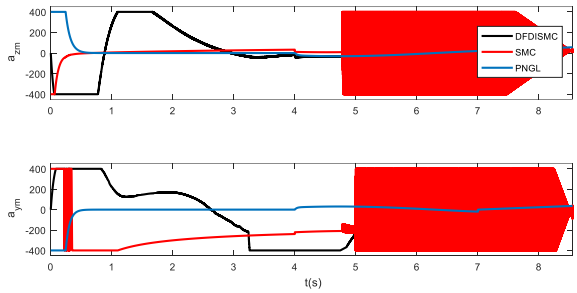

Figure 9. LOS angular rate

Figure 9 shows the interceptor accelerations, and it can be seen that the lateral accelerations are in reasonable scales under the three different guidance laws. In the figure, the chattering effect can be seen for the SMC guidance law, which is undesirable and destructive. In contrast, the chattering effect is eliminated with the proper design of the DFDISMC guidance law, and the lateral accelerations are smooth.

Table 2 presents the Numerical results, including interception time, miss distance, LOS angle error, and interceptor acceleration for two studied cases performed utilizing the three guidance laws.

Table 2. performance comparison of three guidance laws

Cases	Guidance law	Interception time (s)	Miss distance (m)	Error of θ_L (deg)	Error of ϕ_L (deg)	$\int a_{zm}dt$(m/s)	$\int a_{ym}dt$(m/s)
Case 1	DFDISMC	10.581	0.254	0.0058	0.0005	312	345
	SMC	10.593	0.69	0.0068	0.0019	339	356
	PNGL	8.189	0.82	4.789	24.775	280	322
Case 2	DFDISMC	8.512	0.436	0.006	0.001	184	243
	SMC	8.557	0.575	0.007	0.002	202	265
	PNGL	7.469	0.678	4.9	24.9	102	196

Table 2, for case 1, shows that the interception times under the guidance laws of DFDISMC and SMC are approximately equal (10.5 sec). However, the

interception time derived by PNGL law is less (8.2 sec). For the miss distances and LOS angle errors, the DFDISMC guidance law shows better performance, and these values are much less than those under SMC and PNGL. Furthermore, the investigation of cumulative velocity increments shows the proper performance of the DFDISMC method. A similar trend can be seen in case 2. The interception times for DFDISMC and SMC guidance laws are similar. DFDISMC and SMC show much better performance for the LOS angles errors than the PN guidance law. Besides, for the cumulative velocity increments, DFDISMC with 243 m/s shows better performance.

Conclusion

This paper proposed a novel composite guidance law based on dynamic inversion sliding mode control with terminal impact angle constraint. This proposition was made to aid in effectively impacting the interceptor in maneuvering targets. In this paper, a novel composite guidance law based on dynamic inversion sliding mode control was proposed for the interceptor impacting maneuvering targets with a terminal impact angle constraint. Moreover, the finite impact time in desired angles was shown to be rendered true. As was established, the chattering phenomenon is the main disadvantage of the sliding mode control method. Thus, this paper proposes a dynamic form of sliding mode control achieved by employing a second sliding surface. The attainment of the first-order dynamic of the achieved input allows for the chattering problem to be eliminated. Ultimately, the simulation results validated the theoretical theorems. The simulation demonstrated that the DIFTSMC guidance law performed substantially better than both PNGL and SMC methods. In this research, it was assumed that the upper bounds of target accelerations are available. For future studies, estimating target accelerations can be a viable choice.

Declaration of conflicting interests

The author(s) declared no potential conflicts of interest concerning this article's research, authorship, and/or publication.

Acknowledgment

The authors would like to thank Shahid Chamran University of Ahvaz for their financial support.

References

[1] M. Mohiyeddin, S. Behrouz, and B. Tahereh, “Optimal Guidance Law Based on Virtual Sliding Target,” *J. Aerosp. Eng.*, vol. 30, no. 3, p. 4016097, May 2017, doi: 10.1061/(ASCE)AS.1943-5525.0000692.

[2] R. Bardhan and D. Ghose, “Nonlinear Differential Games-Based Impact-Angle-Constrained Guidance Law,” *J. Guid. Control. Dyn.*, vol. 38, no. 3, pp. 384–402, Feb. 2015, doi: 10.2514/1.G000940.

[3] H. Cho, C.-K. Ryoo, A. Tsourdos, and B. White, “Optimal Impact Angle Control Guidance Law Based on Linearization About Collision Triangle,” *J. Guid. Control. Dyn.*, vol. 37, no. 3, pp. 958–964, Mar. 2014, doi: 10.2514/1.62910.

[4] V. Behnamgol, A. R. Vali, and A. Mohammadi, “A new adaptive finite time nonlinear guidance law to intercept maneuvering targets,” *Aerosp. Sci. Technol.*, vol. 68, pp. 416–421, 2017, doi: 10.1016/j.ast.2017.05.033.

[5] H. K. Khalil and J. W. Grizzle, *Nonlinear systems*, vol. 3. Prentice hall Upper Saddle River, NJ, 2002.

[6] Y. Shu and S. Tang, “Integrated Robust Dynamic Inversion Design of Missile Guidance and Control Based on Nonlinear Disturbance Observer,” in *2012 4th International Conference on Intelligent Human-Machine Systems and Cybernetics*, 2012, vol. 2, pp. 42–45, doi: 10.1109/IHMSC.2012.106.

[7] R. Tekin, K. S. Erer, and F. Holzapfel, “Control of Impact Time with Increased Robustness via Feedback Linearization,” *J. Guid. Control. Dyn.*, vol. 39, no. 7, pp. 1682–1689, Apr. 2016, doi: 10.2514/1.G001719.

[8] A. Abaspour, M. Sadeghi, and S. H. Sadati, “Using fuzzy logic in dynamic inversion flight controller with considering uncertainties,” in *2013 13th Iranian Conference on Fuzzy Systems (IFSC)*, 2013, pp. 1–6, doi: 10.1109/IFSC.2013.6675662.

[9] S. R. Kumar, S. Rao, and D. Ghose, “Nonsingular Terminal Sliding Mode Guidance with Impact Angle Constraints,” *J. Guid. Control. Dyn.*, vol. 37, no. 4, pp. 1114–1130, Feb. 2014, doi: 10.2514/1.62737.

[10] J. Song, S. Song, and H. Zhou, “Adaptive nonsingular fast terminal sliding mode guidance law with impact angle constraints,” *Int. J. Control. Autom. Syst.*, vol. 14, no. 1, pp. 99–114, 2016, doi: 10.1007/s12555-014-0155-8.

[11] H. Ji, X. Liu, Z. Song, and Y. Zhao, “Time-varying sliding mode guidance scheme for maneuvering target interception with impact angle constraint,” *J. Franklin Inst.*, vol. 355, no. 18, pp. 9192–9208, 2018, doi: 10.1016/j.jfranklin.2017.01.036.

[12] L. Zhao and Y. Jia, “Finite-time attitude tracking control for a rigid spacecraft using time-varying terminal sliding mode techniques,” *Int. J. Control*, vol. 88, no. 6, pp. 1150–1162, Jun. 2015, doi: 10.1080/00207179.2014.996854.

[13] L. Zhao and Y. Jia, “Neural network-based distributed adaptive attitude synchronization control of spacecraft formation under modified fast terminal sliding mode,” *Neurocomputing*, vol. 171, pp. 230–241, 2016, doi: 10.1016/j.neucom.2015.06.063.

[14] S. Xiong, W. Wang, X. Liu, S. Wang, and Z. Chen, “Guidance law against maneuvering targets with intercept angle constraint,” *ISA Trans.*, vol. 53, no. 4, pp. 1332–1342, 2014, doi: 10.1016/j.isatra.2014.03.007.

[15] S. He, D. Lin, and J. Wang, "Continuous second-order sliding mode based impact angle guidance law," *Aerosp. Sci. Technol.*, vol. 41, pp. 199–208, 2015, doi: 10.1016/j.ast.2014.11.020.

[16] V. Behnamgol, A. R. Vali, and A. Mohammadi, "A new observer-based chattering-free sliding mode guidance law," *Proc. Inst. Mech. Eng. Part G J. Aerosp. Eng.*, vol. 230, no. 8, pp. 1486–1495, Nov. 2015, doi: 10.1177/0954410015612499.

[17] J. Zhao, R. Zhou, and Z. Dong, "Three-dimensional cooperative guidance laws against stationary and maneuvering targets," *Chinese J. Aeronaut.*, vol. 28, no. 4, pp. 1104–1120, 2015, doi: 10.1016/j.cja.2015.06.003.

[18] Y.-Y. Chen, "Robust terminal guidance law design for missiles against maneuvering targets," *Aerosp. Sci. Technol.*, vol. 54, pp. 198–207, 2016, doi: 10.1016/j.ast.2016.03.028.

[19] H. Shin, A. Tsourdos, and K. Li, "A New Three-Dimensional Sliding Mode Guidance Law Variation With Finite Time Convergence," *IEEE Trans. Aerosp. Electron. Syst.*, vol. 53, no. 5, pp. 2221–2232, 2017, doi: 10.1109/TAES.2017.2689938.

[20] Q. Hu, T. Han, and M. Xin, "Three-Dimensional Guidance for Various Target Motions With Terminal Angle Constraints Using Twisting Control," *IEEE Trans. Ind. Electron.*, vol. 67, no. 2, pp. 1242–1253, 2020, doi: 10.1109/TIE.2019.2898607.

[21] C. Man, Z. Zhang, and S. Li, "Two composite guidance laws based on the backstepping control and disturbance observers with autopilot lag," *Trans. Inst. Meas. Control*, vol. 41, no. 10, pp. 2957–2969, Jan. 2019, doi: 10.1177/0142331218821422.

[22] S.-H. Song and I.-J. Ha, "A Lyapunov-like approach to performance analysis of 3-dimensional pure PNG laws," *IEEE Trans. Aerosp. Electron. Syst.*, vol. 30, no. 1, pp. 238–248, 1994, doi: 10.1109/7.250424.

[23] D. Zhou, S. Sun, and K. L. Teo, "Guidance Laws with Finite Time Convergence," *J. Guid. Control. Dyn.*, vol. 32, no. 6, pp. 1838–1846, Nov. 2009, doi: 10.2514/1.42976.

[24] Y. Feng, F. Han, and X. Yu, "Chattering free full-order sliding-mode control," *Automatica*, vol. 50, no. 4, pp. 1310–1314, 2014.

[25] E. Moulay and W. Perruquetti, "Finite time stability and stabilization of a class of continuous systems," *J. Math. Anal. Appl.*, vol. 323, no. 2, pp. 1430–1443, 2006.

[26] J. Liu and X. Wang, *Advanced Sliding Mode Control for Mechanical Systems: Design, Analysis and MATLAB Simulation*. Springer Berlin Heidelberg, 2012.

[27] Y. Feng, X. Yu, and Z. Man, "Non-singular terminal sliding mode control of rigid manipulators," *Automatica*, vol. 38, no. 12, pp. 2159–2167, 2002.

[28] J. Gao, and C. Yuan-Li, "Three-Dimensional Impact Angle Constrained Guidance Laws with Fixed-Time Convergence," *Asian J. Control*, vol. 19, no. 6, pp. 2159–2167, 2017.

[29] P. Zhang and X. Zhang, "A novel adaptive three-dimensional finite-time guidance law with terminal angle constraints for interception of maneuvering targets," *Int. J. Control*, vol. 95, no. 6, pp. 1590–1599, 2022.